

High-temperature ordering of structural vacancies in the cobalt-rich portion of the binary system Co–Ge

N. Audebrand¹, M. Ellner, E.J. Mittemeijer*

Max Planck Institute for Metals Research, Heisenbergstrasse 3, D-70569 Stuttgart, Germany

Received 11 June 2004; accepted 6 July 2004

Abstract

X-ray powder diffraction analysis, macroscopic density measurement and light microscopical methods were used for the investigation of the ordering of structural vacancies in the high-temperature phase Co_3Ge_2 . The heat treated alloy of the composition $\text{Co}_{58}\text{Ge}_{42}$ (bulk specimen: 43 h at 700 °C; powder specimen: 43 h at 700 °C) showed the crystal structure of Co_3Ge_2 : Pearson–Parthé symbol ($hP22-1.7$), space group $P6_3/mmc$, Fe_{2-x}Ge type, $a = 7.7541(8)$ Å, $c = 4.991(1)$ Å. The distribution of structural vacancies as determined for the high-temperature phase Co_3Ge_2 differs from the one for the quasihomologous phase $\text{Ni}_{19}\text{Ge}_{12}$. This effect is caused by the difference in filling of the 3d band for the late transition metals cobalt and nickel.

© 2004 Elsevier B.V. All rights reserved.

Keywords: Transition metal compounds; Structural vacancies; Ordered phases; X-ray diffraction

1. Introduction

Phase diagrams reported for the binary system Co–Ge [1–3] show, in the composition range $0.326 < x_{\text{Ge}} < 0.43$ and at temperatures above 650 °C, only the high-temperature phase Co_5Ge_3 (β) as stable solid phase. This congruently melting berthollidic phase is isotypic with Ni_2In ($hP(6-n)$, $P6_3/mmc$) [4] and possesses a defect structure: the number of structural vacancies increases with increasing valence electron concentration (VEC) and thus increasing mole fraction of germanium [5,6]. In conflict with the phase equilibria reported in [1–3], according to [7] a high-temperature η solid phase would occur additionally for the Co–Ge system in the composition range $0.40 < x_{\text{Ge}} < 0.43$ at temperatures in the range ~ 500 –982 °C. To eliminate the inconsistency in

the knowledge about the phase equilibria in the cobalt-rich portion of the binary system Co–Ge, this study focuses on the crystal structure determination of solid phases occurring around the Co_3Ge_2 composition.

2. Experimental

2.1. Preparation of alloys

Binary mixtures consisting of cobalt (99.9 wt.%; Johnson Matthey) and germanium (99.9999 wt.%; Johnson Matthey) (of mass approximately 3 g) were melted in an induction furnace under 60 kPa argon (Messer–Griesheim 5.0). No significant mass loss was observed upon comparing the weights of the initial amounts of elements and of the final solidified alloyed specimens. For the homogenization heat-treatment, the alloys were put into evacuated and then with argon filled sealed silica ampoules, annealed at 700 °C for 43 h and subsequently water quenched. The homogeneity of specimens was investigated using light microscopical methods with polarized light.

* Corresponding author. Tel.: +49 711 689 3311; fax: +49 711 689 3312.

E-mail address: e.j.mittemeijer@mf.mpg.de (E.J. Mittemeijer).

¹ Present address: Université de Rennes 1, Laboratoire de Chimie du Solide et Inorganique Moléculaire, Groupe de Cristallographie des Poudres et Réactivité des Solides, 263 Avenue du Général Leclerc, F-35042 Rennes Cedex, France.

2.2. X-ray diffraction analysis

For X-ray powder diffraction analysis, bulk heat treated alloys were powdered in a mortar, passed through a sieve (mesh size: 0.05 mm) and annealed (at 700 °C for 43 h) in small evacuated silica tubes to remove the filing induced deformation. Powder diffraction patterns were recorded in a Guinier transmission camera (Enraf-Nonius FR552) using Co $K\alpha_1$ ($\lambda = 1.788965 \text{ \AA}$) and/or Mo K_1 radiation ($\lambda = 0.70930 \text{ \AA}$). Germanium (99.9999 wt.%; Johnson Matthey) was used as an internal calibration standard. The annealed powders were put on a piece of adhesive band. Single coated CEA Reflex 15 film was applied for the Guinier patterns. Integrated intensities of diffraction lines recorded in the Guinier patterns were densitometrically analysed by means of a Line Scanner LS 20 (KEJ Instruments). The powder diffraction lines were indexed by application of the successive dichotomy method (program *DICVOL91* [8]). The unit cell parameters were refined by least-squares fitting using the evaluation program *NBS*AIDS83* [9]. The figures of merit M_N [10] and F_N [11] were determined for the powder diffraction data. Powder diffraction intensities were calculated by means of the program *LAZY PULVERIX* [12].

2.3. Macroscopic density measurement

The density of alloys was measured by means of a gas pycnometer ACCUPYC 1330 (Micromeritics Instrument Corporation) using helium (99.999%: Messer-Griesheim) as gas medium.

3. Results

Guinier patterns (recorded using Co $K\alpha_1$ radiation) of alloys $\text{Co}_{60}\text{Ge}_{40}$ (powder, heat treated at 850° for 10 days, water quenched) and $\text{Co}_{59}\text{Ge}_{41}$ (powder, heat treated at 850° for 6 days, water quenched) showed diffraction lines indicative of the Ni_2In structure type; other diffraction lines did not occur. In contrast with these results, the powder diffraction pattern of the alloy $\text{Co}_{58}\text{Ge}_{42}$ (powder, heat treated at 700 °C for 43 h, water quenched) showed not only the diffraction lines corresponding to the Ni_2In structure type, but additionally new superstructure diffraction lines were detected. The positions of the superstructure and parent structure diffraction lines were commensurable. The superstructure diffraction lines were indexed by means of a hexagonal unit cell four times larger than that of the parent one: $a_H \approx 2a_h$, $c_H \approx c_h$ (a_h and c_h are the unit cell parameters of the initial Ni_2In type unit cell; a_H and c_H are the unit cell parameters of the superstructure unit cell). Guinier patterns recorded for the alloys $\text{Co}_{56.5}\text{Ge}_{43.5}$, $\text{Co}_{55}\text{Ge}_{45}$ and $\text{Co}_{52}\text{Ge}_{48}$ (powders heat treated at 700 °C for 43 h, water quenched) showed diffraction lines of two phases: the phase of the Ni_2In type structure and the CoGe phase (see [13]).

Table 1
Powder diffraction data for the high-temperature phase Co_3Ge_2^a

hkl	$d_c(\text{\AA})$	$d_o(\text{\AA})$	I_o	I_c
010	6.7153	–	–	1
011	4.0058	4.005	1	<1
110	3.8771	3.8835	1	1
020	3.3576	3.3607	3	2
021	2.7859	2.7889	23	25
120	2.5381	2.5405	5	7
002	2.4956	2.4953	5	7
012	2.3392	–	–	<1
121	2.2624	2.2636	6	13
030	2.2384	2.2387	1	1
112	2.0984	2.0985	1	<1
031	2.0424	2.0427	6	12
022	2.0029	2.0038	100	100
220	1.9385	1.9393	87	83
130	1.8625	–	–	<1
122	1.7795	1.7796	3	5
131	1.7450	1.7451	1	3
040	1.6788	1.6789	2	1
032	1.6663	1.6661	1	1
013	1.6149	–	–	<1
041	1.5912	1.5910	4	3
230	1.5406	1.5403	1	2
222	1.5309	1.5307	2	4
132	1.4926	–	–	1
023	1.4907	1.4906	3	4
231	1.4721	1.4717	1	2
140	1.4654	–	–	<1
141	1.4060	1.4055	3	5

^a $hP(22-1.7)$, $P6_3/mmc$, $a_H = 7.7541(8) \text{ \AA}$, $c_H = 4.991(1) \text{ \AA}$.

The unit cell parameters, determined from the Guinier pattern (Co $K\alpha_1$ radiation) of the alloy $\text{Co}_{58}\text{Ge}_{42}$ (bulk alloy, heat treated at 700 °C for 43 h, powder, heat treated at 700 °C for 43 h, water quenched) are: $a_H = 7.7541(8) \text{ \AA}$ and $c_H = 4.991(1) \text{ \AA}$; $2c_H/a_H = 1.287$. The figures of merit were: $M_{20} = 72$ and $F_{21} = 47$ (0.0161, 28). The macroscopic density was determined as $8.377(1) \text{ Mg m}^{-3}$, which corresponds to a number of atoms in the superstructure unit cell of the high-temperature phase, (in the following denoted by Co_3Ge_2), N^C , equal to 20.3. The powder diffraction data obtained for the Co_3Ge_2 phase have been gathered in Table 1. The crystal structure proposed for the Fe_{2-x}Ge (η) phase [7], standardized by Parthé et al. [14], and adapted for the number of atoms in the unit cell, $N^C = 20.3$, was employed for the calculation of the powder diffraction intensities: $hP(22-1.7)$, $P6_3/mmc$, $2\text{Co}(a)$, $6\text{Co}(g)$, $0.72 \times 6\text{Co}(h)$ (0.1615, 0.3230, 1/4), $2\text{Ge}(c)$, $6\text{Ge}(h)$ (0.8078, 0.6156, 1/4). The satisfactory correspondence of observed and calculated intensities, as shown in Table 1, demonstrates that the crystal structure of Co_3Ge_2 is isotypic with the Fe_{2-x}Ge (η) crystal structure.

Light microscopical investigation of alloys $\text{Co}_{58}\text{Ge}_{42}$ and $\text{Co}_{57}\text{Ge}_{43}$ (bulk alloys, heat treated at 700 °C for 3 days) in polarized light showed large pleochroitic grains. Neither multiple twinning [15] nor formation of a domain structure [16] could be observed for these ordered alloys.

4. Discussion

The present investigation confirms the occurrence of a stable, high-temperature, ordered phase η in the binary system Co–Ge. Hence, the phase equilibria around the stoichiometry Co_3Ge_2 as given originally in [17] and later unrestrictedly adopted in the compendia [1–3] are erroneous.

The proposal given in [7] for the (schematic) phase diagram Co–Ge in the composition range of the Co_3Ge_2 phase shows a topology analogous to that observed for the Ni–Ge system around the Ni_3Ge_2 composition, also comprising a stable, high-temperature, ordered Ni_2In superstructure. In other nickel-containing systems—Ni–Ga and Ni–In—ordered superstructures homeotypical with Ni_2In occur at $0.41 \leq x_{\text{Ga,In}} \leq 0.42$ [6,18].

Evidently, as demonstrated by the above results, a superstructure occurs for $\text{Co}_{58}\text{Ge}_{42}$ and is absent for $\text{Co}_{59}\text{Ge}_{41}$ and alloys richer in Ge. Light microscopical analysis of these alloys (heat treated at 700°C for 3 days) did not reveal any microstructure difference. This result parallels similar observations made for the Ni–Ge system around the Ni_3Ge_2 composition [6,15].

In contrast to the observations made for the high-temperature ordered phases Co_3Ge_2 (this work; see end of Section 3) and $\text{Ni}_{19}\text{Ge}_{12}$ [15], significant multiple twinning was observed for the low-temperature ordered phase Ni_5Ge_3 [15]. In the latter case, the ordering of the structural vacancies is accompanied with considerable symmetry change— $\text{Ni}_{2-x}\text{Ge}(\text{h})$ ($P6_3/mmc$, defect Ni_2In type) \rightarrow Ni_5Ge_3 ($C2$, Ni_5Ge_3 type)—causing the lattice distortions characterized by: $3b_{\text{Ni}_5\text{Ge}_3}/a_{\text{Ni}_5\text{Ge}_3} = 1.730 < \sqrt{3}$ (the “orthorhombical distortion”) and $\arctan[c_{\text{Ni}_5\text{Ge}_3} \sin \beta_{\text{Ni}_5\text{Ge}_3} / (c_{\text{Ni}_5\text{Ge}_3} \cos \beta_{\text{Ni}_5\text{Ge}_3} - a_{\text{Ni}_5\text{Ge}_3}/3)] = 89.84^\circ < 90^\circ$ (the “monoclinical distortion”); cf. [15].

For the high-temperature phases $\text{Co}_2\text{Ge}(\text{h})$ (no superstructure) and Co_3Ge_2 (superstructure), the composition dependence of both the axial ratio c/a and the volume of the parent structure (Ni_2In type) unit cell is shown in Fig. 1. The distinct change in slope of the curve at $x_{\text{Ge}} \sim 0.39$ is indicative of the occurrence of a superstructure for compositions $x_{\text{Ge}} > 0.40$. A similar phenomenon was observed also at the boundary of the phase regions for $\text{Ni}_2\text{Ge}(\text{h})/\text{Ni}_{19}\text{Ge}_{12}$ and Ni_3Ge_2 [6,15].

Despite the occurrence of some similarities in behaviour of the high-temperature ordered superstructures $\text{Ni}_{19}\text{Ge}_{12}$

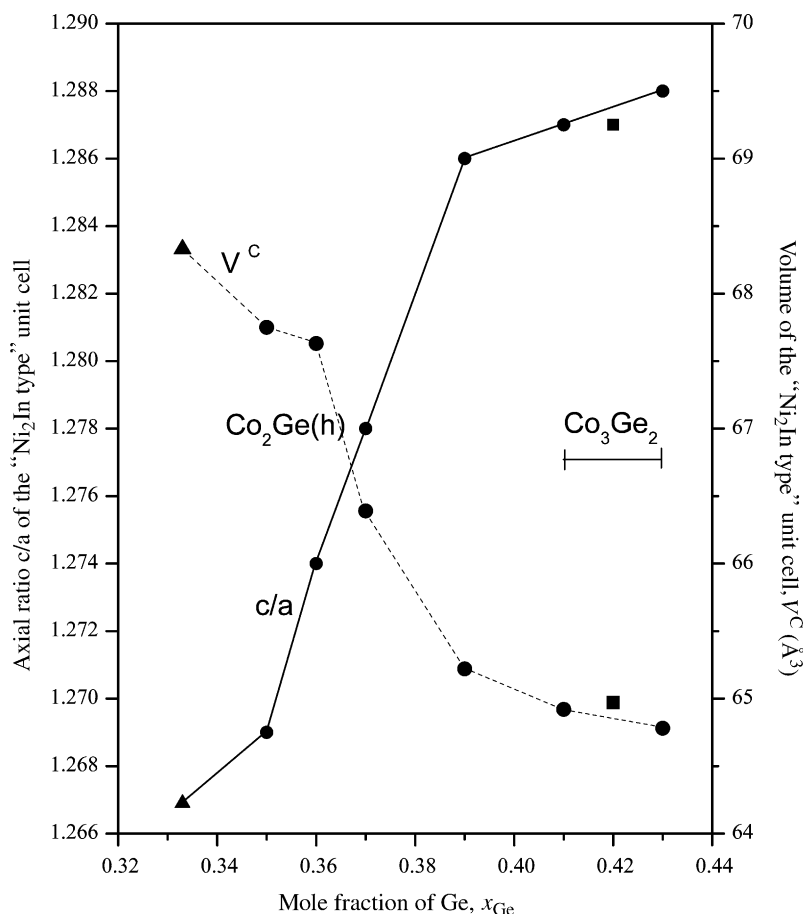


Fig. 1. Composition dependence of the axial ratio c/a as well as of the unit cell volume, V^C , for the parent Ni_2In structure of the high-temperature phases $\text{Co}_2\text{Ge}(\text{h})$ and Co_3Ge_2 . Data according to [6] (●), [22] (▲) and this investigation (■).

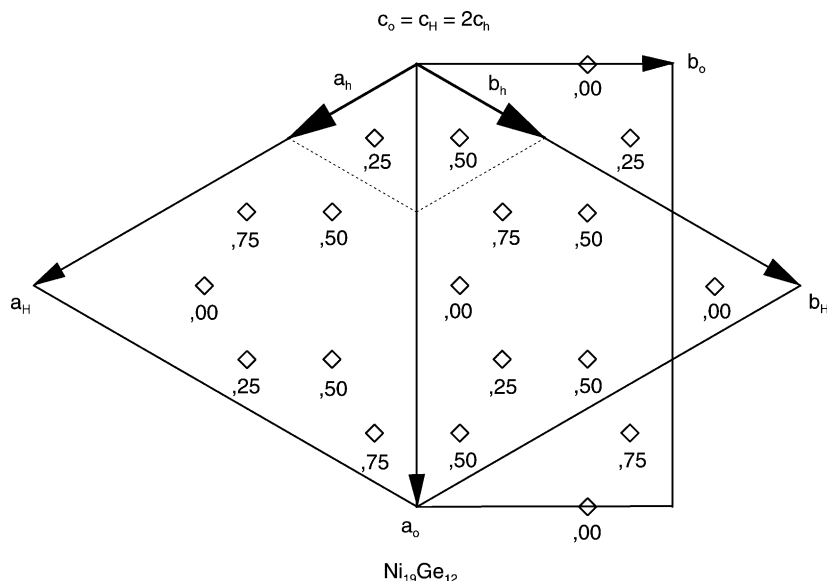


Fig. 2. Distribution of structural vacancies (◊) in the “trigonal prismatic holes” of the Ni₂In parent structure for the high-temperature phase Ni₁₉Ge₁₂. Projection of lattice sites on (001) plane. The orthorhombic unit cell, $a_o \approx 3a_h + 3b_h$, $b_o \approx -a_h + b_h$, $c_o \approx 2c_h$ [15] has been indicated too.

and Co₃Ge₂, their germanium contents are different and they contain different number of atoms in the “Ni₂In type” unit cell: the crystal structures of Ni₁₉Ge₁₂ and Co₃Ge₂ are quite different. The relationship between the pseudohexagonal superstructure-unit cell (H) of phase Ni₁₉Ge₁₂ ($x_{Ge} \sim 0.385$) and the hexagonal parent structure unit cell (h) is given by the equations: $a_H \approx 3a_h$, $c_H \approx 2c_h$ [15]. Concerning the periodicity in the [00 1]-direction, Ni₁₉Ge₁₂ represents a “two layer” type of the Ni₂In-superstructure. For the phase Co₃Ge₂ phase ($x_{Ge} > 0.40$) the relationship to the Ni₂In type unit cell is: $a_H \approx 2a_h$, $c_H \approx c_h$ (cf. Section 3); Co₃Ge₂ represents thereby, in the previous way of looking (periodicity in the [00 1]-direction), an “one layer” type of the Ni₂In-superstructure.

For the ordered high-temperature phase Ni₁₉Ge₁₂, the locations of the structural vacancies are shown (according to [15]) in Fig. 2. Clearly, in terms of the Ni₂In type parent structure [14], structural vacancies occur exclusively in the position 2(d) of the space group *P6₃/mmc*. A similar kind of structural-vacancy distribution occurs also in the nickel-containing (low-temperature) phases Ni₅Ge₃ [15] and Ni₃Sn₂ [19], which both are homeotypes of the Ni₂In structure.

The locations of the structural vacancies in the high-temperature hexagonal ordered phase Co₃Ge₂ (Fe_{2-x}Ge type) are shown (according to [7,14]) in Fig. 3. In this superstructure, the structural vacancies also occur (with reference to the the Ni₂In type parent structure [14]) on the position 2(d) of the space group *P6₃/mmc*, but their distribution over these positions is different from that for the superstructures Ni₅Ge₃, Ni₁₉Ge₁₂ and Ni₃Sn₂: some of these “trigonal prismatic holes” are not fully, but only *partially* occupied by cobalt atoms. With respect to the Fe_{2-x}Ge structure (*P6₃/mmc*) [14], the position 2(d) is completely empty;

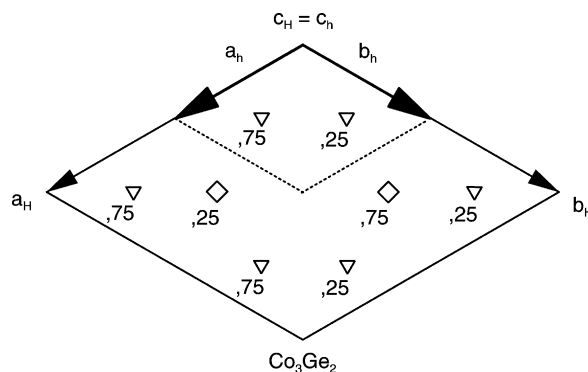


Fig. 3. Distribution of structural vacancies in the “trigonal prismatic holes” of the Ni₂In parent structure for the high-temperature phase Co₃Ge₂. Projection of lattice sites on (001) plane. Symbols: “trigonal prismatic holes” showing structural vacancies exclusively (◊); “trigonal prismatic holes” showing structural vacancies only partially (28%) (∇).

the atomic position 6(h) is partially filled by cobalt atoms (cf. Section 3). The “occupation factor for vacancies” in the position 6(h) is equal to 0.28 (cf. symbol ∇ in Fig. 3).

The reason that both quasihomologous phases, Co₃Ge₂ and Ni₁₉Ge₁₂, occur at different germanium compositions and that they show different number of atoms in the (Ni₂In type) parent structure unit cell, may be ascribed, according to the Norbury rule [20,21], to the different fillings of the d-bands of both quasihomologous transition metals (cobalt: 3d⁷4s² and nickel: 3d⁸4s²).

5. Conclusion

- (i) A stable high-temperature ordered phase Co₃Ge₂ exists. The phase diagram of the binary system Co–Ge as

shown in existing compilations in the literature has to be modified accordingly.

- (ii) The crystal structure of the Co_3Ge_2 phase is isotypical with Fe_{2-x}Ge , $hP(22-1.7)$, $P6_3/mmc$.
- (iii) In contrast with the quasihomologous phase $\text{Ni}_{19}\text{Ge}_{12}$, some (trigonal prismatic) lattice positions for the cobalt atoms are in the Co_3Ge_2 phase occupied partially.
- (iv) The structural differences between Co_3Ge_2 and $\text{Ni}_{19}\text{Ge}_{12}$ are ascribed to the different fillings of the d-bands of the quasihomologous transition elements cobalt and nickel.

References

- [1] T.B. Massalski, H. Okamoto, P.R. Subramanian, L. Kacprzak, Binary Alloy Phase Diagrams, second ed., vol. 2, ASM International, The Materials Information Society, OH, 1990.
- [2] K. Ishida, T. Nishizawa, J. Phase Equilib. 12 (1991) 77.
- [3] B. Predel, Phasengleichgewichte, kristallographische und thermodynamische Daten binärer Legierungen, Band 5c, in Landolt Börnstein, Neue Serie, Springer Verlag, Berlin, 1993.
- [4] F. Laves, H. Wallbaum, Z. angew. Mineral 4 (1941–1942) 17.
- [5] T.P. Agalakova, V.L. Zagrjashkij, P.V. Geld, Izv. Akad. Nauk SSSR, Neorg. Mater. 9 (1973) 1180.
- [6] M. Ellner, J. Less-Common Met. 48 (1976) 21.
- [7] B. Malaman, J. Steinmetz, B. Roques, J. Less-Common Met. 75 (1980) 155.
- [8] A. Boulitf, D. Louër, J. Appl. Cryst. 24 (1991) 987.
- [9] A.D. Mighell, C.R. Hubbard, J.K. Stalick, NBS*AIDS80. A Fortran Program for Crystallographic Data Evaluation (US Technical Note 1141), NBS Washington, Washington D.C., 1981.
- [10] D.M. de Wolf, J. Appl. Cryst. 5 (1968) 108.
- [11] G.S. Smith, R.L. Snyder, J. Appl. Cryst. 12 (1979) 60.
- [12] K. Yvon, W. Jeitschko, E. Parthé, J. Appl. Cryst. 20 (1977) 73.
- [13] N. Audebrand, M. Ellner, E.J. Mittemeijer, Powder Diffr. 15 (2000) 120.
- [14] E. Parthé, L. Gelato, B. Chabot, M. Penzo, K. Cenzual, R. Gladyshevskii, TYPIX, Standardized Data and Crystal Chemical Characterization of Inorganic Structures, vol. 4, Springer Verlag, Berlin, 1994.
- [15] M. Ellner, T. Gödecke, K. Schubert, J. Less-Common Met. 24 (1971) 23.
- [16] K.Ch. Jain, M. Ellner, K. Schubert, Z. Metallkd. 63 (1972) 456–461.
- [17] P. Feschotte, A. Dayer, J. Less-Common Met. 72 (1980) 51.
- [18] M. Ellner, S. Bhan, K. Schubert, J. Less-Common Met. 19 (1969) 245.
- [19] P. Brand, Z. Anorg. Allg. Chem. 353 (1967) 270.
- [20] A.L. Norbury, J. Inst. Met. 65 (1939) 355.
- [21] K. Schubert, Kristallstrukturen zweikomponentiger Phasen, Springer-Verlag, 1964.
- [22] N. Audebrand, M. Ellner, E.J. Mittemeijer, J. Alloys Compd. 353 (2003) 228.